Molecular Therapy
Methods & Clinical Development
Original Article

Rapamycin Rescues Age-Related Changes in Muscle-Derived Stem/Progenitor Cells from Progeroid Mice

Yohei Kawakami,[1,4,6] William S. Hambright,[2,3,6] Koji Takayama,[1,4] Xiaodong Mu,[1,2,3] Aiping Lu,[1,2,3] James H. Cummins,[1] Tomoyuki Matsumoto,[4] Takashi Yurube,[4] Ryosuke Kuroda,[4] Masahiro Kurosaka,[4] Freddie H. Fu,[1] Paul D. Robbins,[5] Laura J. Niedernhofer,[5] and Johnny Huard[3]

[1]Stem Cell Research Center, Department of Orthopaedic Surgery, University of Pittsburgh, Pittsburgh, PA 15213, USA; [2]Department of Orthopaedic Surgery, University of Texas Health Science Center at Houston, Houston, TX 77054, USA; [3]Steadman Philippon Research Institute, Vail, CO 81657, USA; [4]Department of Orthopaedic Surgery, Kobe University Graduate School of Medicine, Kobe 650-0017, Japan; [5]Department of Biochemistry, Molecular Biology and Biophysics, Institute on Biology of Aging and Metabolism, University of Minnesota, Minneapolis, MN 55455, USA

Aging-related loss of adult stem cell function contributes to impaired tissue regeneration. Mice deficient in zinc metalloproteinase STE24 (*Zmpste24*$^{-/-}$) exhibit premature age-related musculoskeletal pathologies similar to those observed in children with Hutchinson-Gilford progeria syndrome (HGPS). We have reported that muscle-derived stem/progenitor cells (MDSPCs) isolated from *Zmpste24*$^{-/-}$ mice are defective in their proliferation and differentiation capabilities in culture and during tissue regeneration. The mechanistic target of rapamycin complex 1 (mTORC1) regulates cell growth, and inhibition of the mTORC1 pathway extends the lifespan of several animal species. We therefore hypothesized that inhibition of mTORC1 signaling would rescue the differentiation defects observed in progeroid MDSPCs. MDSPCs were isolated from *Zmpste24*$^{-/-}$ mice, and the effects of mTORC1 on MDSPC differentiation and function were examined. We found that mTORC1 signaling was increased in senescent *Zmpste24*$^{-/-}$ MDSPCs, along with impaired chondrogenic, osteogenic, and myogenic differentiation capacity versus wild-type MDSPCs. Interestingly, we observed that mTORC1 inhibition with rapamycin improved myogenic and chondrogenic differentiation and reduced levels of apoptosis and senescence in *Zmpste24*$^{-/-}$ MDSPCs. Our results demonstrate that age-related adult stem/progenitor cell dysfunction contributes to impaired regenerative capacities and that mTORC1 inhibition may represent a potential therapeutic strategy for improving differentiation capacities of senescent stem and muscle progenitor cells.

INTRODUCTION

The molecular basis behind the process of aging and age-related degenerative changes is still unclear; however, it is believed that these changes may be the result of time-dependent accumulation of stochastic molecular and cellular damage.[1,2] Murine models of progeroid syndromes have been studied extensively with the aim of elucidating the fundamental mechanisms that drive aging.[3] Lamin A, which is generated after cleavage of the carboxylic acid group of prelamin A via the zinc metalloproteinase STE24 (ZMPSTE24), is a nuclear envelope protein that provides structural support to the nucleus and is involved in various cellular processes, such as gene expression and DNA replication.[4,5] Through inhibition of *Zmpste24* expression, prelamin A accumulates within the nuclear envelope, resulting in nuclear blebbing, a hallmark feature of Hutchinson Gilford Progeria Syndrome (HGPS).[6,7] *Zmpste24*$^{-/-}$ mice demonstrate a spontaneous onset of premature aging with related physiological and phenotypical changes to the musculoskeletal system, such as weight loss, spontaneous fractures, cardiomyopathy, skeletal muscle atrophy, and weakness—all of which are characteristics of HGPS.[6,8] Prelamin A is involved in the early stages of differentiation of the immortalized mouse myoblast cell line C2C12,[9] with myoblasts expressing a mutated lamin A having a reduced capacity to undergo myogenic differentiation.[10]

Muscle-derived stem/progenitor cells (MDSPCs) are multipotent cells isolated from postnatal skeletal muscle through an established preplating technique.[11–13] They exhibit many important features, including long-term proliferation/self-renewing ability, resistance to oxidative and inflammatory stresses, and the potential for multi-lineage differentiation and self-renewal.[12] MDSPCs can improve the regeneration capacity of both bone and muscle (skeletal and cardiac) through the promotion of angiogenesis.[11,14–16] Although adult stem cells are essential in the maintenance of normal tissue function, these cells are also known to undergo an age-related decline in both number and function, similar to other somatic cell types.[17,18] MDSPCs isolated from *Zmpste24*$^{-/-}$ mice have reduced proliferation and myogenic differentiation capacities when compared to wild-type

Received 12 May 2019; accepted 14 May 2019;
https://doi.org/10.1016/j.omtm.2019.05.011.

[6]These authors contributed equally to this work.

Correspondence: Johnny Huard, PhD, Steadman Philippon Research Institute, 181 West Meadow Drive, Vail, CO 81657, USA.
E-mail: jhuard@sprivail.org

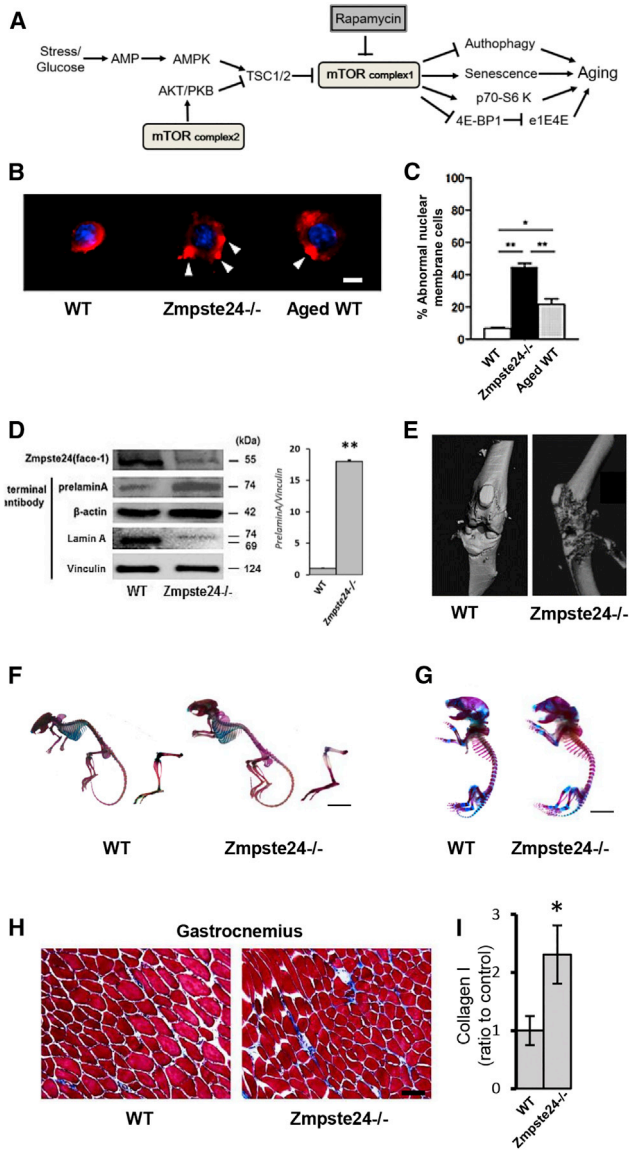

Figure 1. Prelamin A Processing and Gross Musculoskeletal Pathology in *Zmpste24*$^{-/-}$ MDSPCs

(A) Schematic representation of the mTORC1 pathway and its regulation via rapamycin treatment in *Zmpste24*$^{-/-}$ MDSPCs. Arrows indicate activating events; perpendicular lines indicate inhibitory events. mTOR exists in two complexes: mTORC1 containing RAPTOR and mTORC2 containing RICTOR. Down-stream effectors of mTORC1 include p70/S6K regulation of cell proliferation, mRNA translation, and protein synthesis. mTOR is regulated by PI3K and AKT. (B) Representative immunohistochemical staining with anti-lamin A antibodies. Original magnification, ×400. Scale bar, 10 μm. Arrowhead, abnormality in the nuclear membrane. (C) Percentage of abnormal nuclei among cells (*$p < 0.05$, **$p < 0.001$). (D) Western blot analysis to measure the expression of the C-terminal prelamin A and lamin A in WT and *Zmpste24*$^{-/-}$ MDSPCs, relative to the expression of β-actin or vinculin. (E) Representative micro-CT images of bone microarchitecture in knee joint of 8-week-old *Zmpste24*$^{-/-}$ mice. (F and G) Skeletal preparations of 8-week-old (F) and postnatal day 2 (G) *Zmpste24*$^{-/-}$ mice double stained with Alizarin red (bone) and Alcian blue (cartilage). Scale bars, 8 mm. (H and I) Masson's-trichrome-stained gastrocnemius muscle (H) indicating significant levels of fibrosis in 8-week-old *Zmpste24*$^{-/-}$ mice versus age-matched WT animals (I) (*$p < 0.05$). Scale bar, 100 μm.

(WT) MDSPCs.[19] Similarly, the *Ercc1*$^{-/\Delta}$ progeria mouse model of XPF-ERCC1 (XFE) nuclease, with accelerated aging due to endogenous DNA damage, has dysfunctional MDSPCs.[17] The XPF-ERCC1 nuclease is involved in nucleotide excision repair, inter-strand cross-link repair, and repair of double-strand breaks.[20]

mTORC1, also known as mammalian target of rapamycin complex 1 or mechanistic target of rapamycin complex 1, functions as a nutrient/energy/redox sensor and controls protein synthesis (Figure 1A).[21–23] mTORC1 comprises mTOR and the regulatory-associated proteins RAPTOR, MLST8, PRAS40, and DEPTOR.[21,22,24] Downstream mTORC1 effectors including p70/ribosomal S6 kinase (p70/S6K) regulate cell growth and proliferation, as well as protein synthesis.[21–23] Inhibition of mTORC1 with rapamycin also significantly extends the lifespan of genetically heterogeneous mice.[25] Both protein synthesis and autophagy are considered critical in regulation of the mammalian lifespan by mTORC1.[26] Mice deficient in lamin A have been found to have enhanced mTORC1 signaling, specifically in tissues linked to HGPS pathology, including cardiac and skeletal muscle.[27] Furthermore, rapamycin has been found to reverse elevated mTORC1 signaling in lamin-A-deficient mice, rescue cardiac and skeletal muscle function, and extend lifespan.[27] mTORC1 signaling pathways also are activated in MDSPCs from progeroid *Ercc1*$^{-/\Delta}$ mice, and inhibition of mTORC1 with rapamycin promotes autophagy and improves their myogenic differentiation capacity.[28]

Given that stem cell depletion and loss of function with age may limit musculoskeletal tissue regeneration due to reduction in the multi-differentiation potential of adult stem cells, we investigated the impact of premature aging on the multi-lineage differentiation capacity of MDSPCs in ZMPSTE24-deficient (*Zmpste24*$^{-/-}$) mice. We also examined the effects of mTORC1 inhibition on dysfunctional *Zmpste24*$^{-/-}$ MDSPCs with respect to the aging process. Our results demonstrate that age-related adult stem/progenitor cell dysfunction contributes to impaired regenerative capacities, suggesting that mTORC1 inhibition represents a potential therapeutic strategy for improving differentiation capacities of senescent stem and progenitor cells.

RESULTS

MDSPCs from Progeroid *Zmpste24*$^{-/-}$ Mice Exhibit Defective Prelamin A Processing and Musculoskeletal Pathology

To determine whether the defect in lamin processing[7,29] affects stem/progenitor cells, MDSPCs isolated from 8-week-old WT and *Zmpste24*$^{-/-}$ mice were evaluated for their expression and distribution of prelamin A and processed lamin A. Immunohistochemical staining for lamin A revealed that abnormal cell nuclei, as defined by the presence of lobulations at their surfaces, were found in the *Zmpste24*$^{-/-}$ MDSPCs when compared to WT MDSPCs, as well as MDSPCs derived from aged WT mice where nuclear lobulations

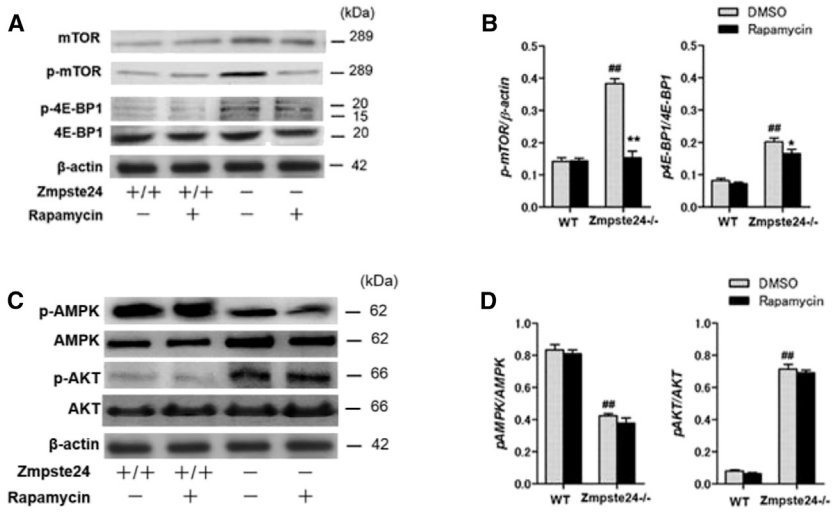

Figure 2. Elevated mTORC1 Activity in *Zmpste24*$^{-/-}$ MDSPCs

(A) Representative western blots indicating mTORC1, p-mTORC1, and p-4E-BP1 expression levels in MDSPCs isolated from *Zmpste24*$^{-/-}$ and WT mice, cultured with and without rapamycin. (B) Quantification of western blots (##p < 0.001 versus WT DMSO; *p < 0.05, **p < 0.001 versus *Zmpste24*$^{-/-}$ DMSO). (C) Representative image of western blots indicating p-AMPK and p-AKT expression in MDSPCs isolated from *Zmpste24*$^{-/-}$ and WT mice, cultured with and without rapamycin. (D) Quantification of p-AMPK and p-AKT expression relative to the expression of β-actin (##p < 0.001 versus WT DMSO). All immunoblots are representative of experiments with similar results (n = 4).

are known to occur (age-matched WT versus *Zmpste24*$^{-/-}$, p < 0.001; 8-week-old WT versus 24-month-old WT, p < 0.05; *Zmpste24*$^{-/-}$ versus aged WT, p < 0.001; Figures 1B and 1C). Further, using antibodies specific for the C-terminal region of prelamin A and lamin A specifically, an increased accumulation of prelamin A and increased band intensity for lamin A at 74 kDa (indicating more unprocessed prelamin A) were found in the *Zmpste24*$^{-/-}$ MDSPCs when compared to the WT MDSPCs (Figure 1D). Thus, the observed dysfunctional processing of prelamin A in Zmpste24-deficient MDSPCs is consistent with previous reports.[6,19,30]

We also examined the effect of *Zmpste24* deletion on skeletal growth and muscle health. Micro computed tomography (micro-CT) of knee joint and skeletal preparations of 8-week-old *Zmpste24*$^{-/-}$ mice indicated bone fragility and rudimentary bone (Figures 1E and 1F), although no obvious skeletal abnormalities (joint formation or subchondral bone) were observed in fetal *Zmpste24*$^{-/-}$ preparations (Figure 1G). Further, skeletal muscle sections collected from adult *Zmpste24*$^{-/-}$ mice showed significantly more collagen 1 deposition, suggesting elevated fibrosis in the progeroid animals (Figure 1H and 1I). Taken together, *Zmpste24*$^{-/-}$ mice and their isolated MDSPCs exhibit pathological symptoms similar to those found in patients with HGPS at the cellular and tissue level.[29]

MDSPCs from Progeroid *Zmpste24*$^{-/-}$ Mice Have Elevated mTORC1 Activation

To test our hypothesis that dysregulation of mTORC1 signaling contributes to the age-related dysfunction seen in MDSPCs isolated from progeroid *Zmpste24*$^{-/-}$ mice, phosphorylation of both downstream and upstream signaling components of the mTORC1 pathway were analyzed by western blot. The expression of phosphorylated mTORC1 (p-mTORC1, Ser2448) and phosphorylated 4E-binding protein 1 (p-4E-BP1), both of which are mTORC1 substrates, was increased in *Zmpste24*$^{-/-}$ MDSPCs compared to age-matched WT MDSPCs (p-mTORC1, p-4E-BP1, p < 0.001; Figures 2A and 2B). As expected, rapamycin treatment restored the levels of p-mTORC1 and p-4E-BP1, when compared to vehicle treatment in *Zmpste24*$^{-/-}$ cells (p-mTORC1, p < 0.001; p-4E-BP1, p < 0.05; Figures 2A and 2B). Regarding upstream signaling components of mTORC1, expression of phosphorylated adenosine monophosphate-activated protein kinase (p-AMPK) was significantly decreased, whereas expression of phosphorylated protein kinase B (p-AKT) was significantly increased in the *Zmpste24*$^{-/-}$ MDSPCs, when compared to the WT MDSPCs (p-AMPK and p-AKT, p < 0.001; Figures 2C and 2D). No significant differences were found in levels of these upstream signaling components in *Zmpste24*$^{-/-}$ or WT MDSPCs after rapamycin treatment (Figures 2C and 2D).

Rapamycin Decreases Apoptosis in Progeroid *Zmpste24*$^{-/-}$ MDSPCs

Some adult stem cell populations are dramatically affected by stress, leading to increased apoptosis.[31] We used the terminal deoxynucleotidyl transferase 2′-deoxyuridine, 5′-triphosphate (dUTP) nick-end labeling (TUNEL) assay to determine the extent of apoptosis in progeroid and WT MDSPCs. The percentage of TUNEL-positive (apoptotic) cells in the *Zmpste24*$^{-/-}$ MDSPCs was significantly higher than that in the WT MDSPCs (p < 0.001; Figures 3A and 3B). Rapamycin treatment reduced the percentage of TUNEL-positive cells in *Zmpste24*$^{-/-}$ MDSPCs (p < 0.001; Figures 3A and 3B). Furthermore, increased expression of cleaved poly ADP-ribose polymerase (PARP), an apoptosis marker, was detected in the progeroid *Zmpste24*$^{-/-}$ MDSPCs relative to the WT MDSPCs, and rapamycin treatment also reduced the expression of PARP in *Zmpste24*$^{-/-}$ MDSPCs (Figures 3C and 3D). Thus, rapamycin treatment reduced levels of apoptosis in *Zmpste24*$^{-/-}$ MDSPCs.

Rapamycin Decreases Senescence Markers of Progeroid *Zmpste24*$^{-/-}$ MDSPCs with no Effect on Cellular Proliferation

Cell cycle arrest is an indicator of senescence. *Zmpste24*$^{-/-}$ MDSPCs exhibited increased expression of the cyclin-dependent kinase inhibitor proteins p16 and p21 compared to WT MDSPCs (p < 0.001; Figures 4A and 4B). Accordingly, *Zmpste24*$^{-/-}$ MDSPCs were also

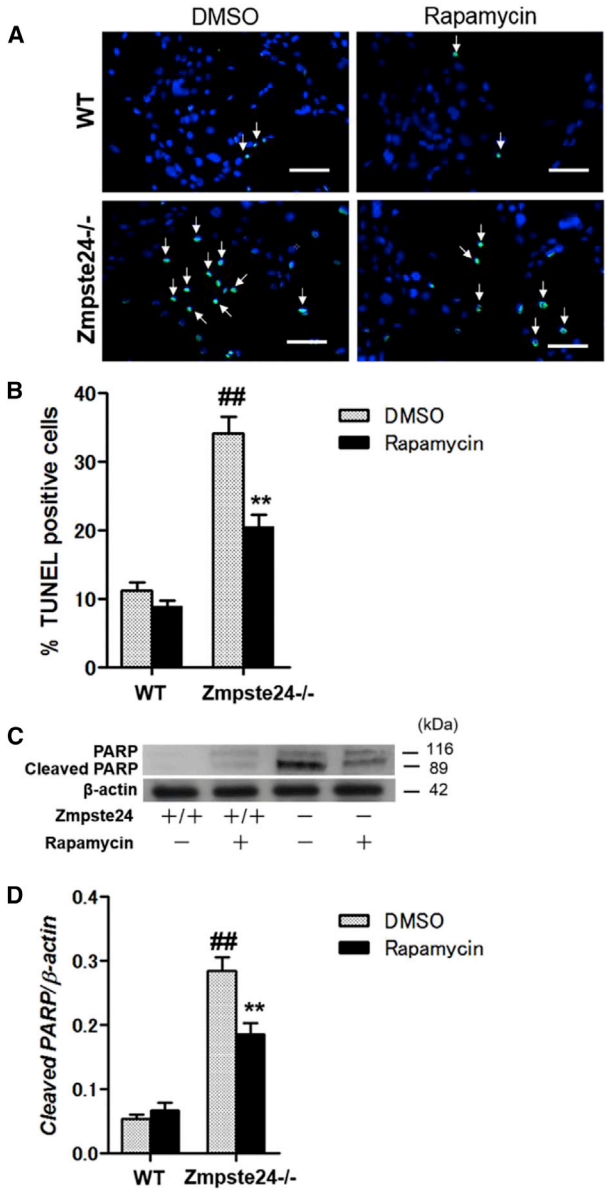

Figure 3. Rapamycin's Effect on Apoptosis in *Zmpste24*$^{-/-}$ MDSPCs

(A) Representative TUNEL images indicating apoptotic cell death of MDSPCs isolated from *Zmpste24*$^{-/-}$ and WT mice, cultured with and without rapamycin. Scale bar, 50 μm. Arrow, TUNEL-positive, apoptotic (green) cells. (B) Percentage of TUNEL-positive cells reported from images obtained from four independent MDSPC populations (##p < 0.001 versus WT DMSO; **p < 0.001 versus *Zmpste24*$^{-/-}$ DMSO). (C) Representative western blots showing expression of the apoptosis-related marker, cleaved PARP, in MDSPCs isolated from *Zmpste24*$^{-/-}$ and WT mice, cultured with and without rapamycin. (D) Quantification of cleaved PARP levels relative to β-actin (n = 4; ##p < 0.001 versus WT DMSO; **p < 0.001 versus *Zmpste24*$^{-/-}$ DMSO).

found to have reduced proliferative capacity versus WT MDSPCs ($p < 0.001$; Figure 4C). However, although rapamycin reduced the expression of p16 and p21 (p21, $p < 0.001$; p16, $p < 0.05$; Figures 4A and 4B), it did not restore the proliferative capacity of either *Zmpste24*$^{-/-}$ or WT MDSPCs (Figure 4C). Cellular senescence is also characterized by elevated β-galactosidase activity.[32] The percentage of senescence-associated β-galactosidase (SA-β-gal)-positive cells among the *Zmpste24*$^{-/-}$ MDSPCs was found to be significantly higher than that of WT MDSPCs ($p < 0.001$; Figure 4D). Importantly, rapamycin treatment significantly reduced the percentage of SA-β-gal-positive cells in the *Zmpste24*$^{-/-}$ MDSPC population ($p < 0.001$; Figure 4D). Overall, these data demonstrate that rapamycin treatment reduces cellular senescence markers in progeroid *Zmpste24*$^{-/-}$ MDSPCs.

Rapamycin Improves the Myogenic Potential of Progeroid *Zmpste24*$^{-/-}$ MDSPCs

To determine whether the myogenic differentiation capacity of the progeroid *Zmpste24*$^{-/-}$ MDSPCs was affected by rapamycin treatment, progeroid and WT cell populations were each cultured to confluence, transferred to differentiation medium (low serum containing medium), and then immunostained to detect the terminal myogenic differentiation marker fast myosin heavy chain (f-MyHC). Independent of rapamycin treatment, the WT MDSPCs fused to form elongated multinucleated myotubes expressing f-MyHC (Figure 5A). In contrast, the *Zmpste24*$^{-/-}$ MDSPCs formed significantly fewer f-MyHC-expressing cells than did WT MDSPCs, suggesting an impaired myogenic differentiation capacity ($p < 0.001$; Figures 5A and 5B). Although not all the cells differentiated into myotubes, rapamycin significantly improved the myogenic differentiation capacity of the *Zmpste24*$^{-/-}$ MDSPCs ($p < 0.001$; Figures 5A and 5B). Impaired differentiation of *Zmpste24*$^{-/-}$ MDSPCs was also confirmed by measuring the mRNA expression levels of two myogenic differentiation markers, *desmin* and myosin heavy chain (*MyHC*) by qPCR. *MyHC* is a differentiation marker of skeletal muscle, and *desmin* is expressed at early stages of myogenic differentiation and is continuously expressed until near-terminal differentiation.[33] The expression level of *desmin* and *MyHC* in the MDSPCs isolated from the progeroid *Zmpste24*$^{-/-}$ mice were significantly reduced compared to those of the WT MDSPCs (*MyHC*, $p < 0.001$; desmin, $p < 0.001$; Figure 5C and 5D). The expression of *desmin* was significantly upregulated in *Zmpste24*$^{-/-}$ MDSPCs after rapamycin treatment. However, although a trend was present, no significant change in *MyHC* expression was found after rapamycin treatment (*MyHC*, $p = 0.455$; *desmin*, $p < 0.05$; Figures 5C and 5D).

Rapamycin Improves the Chondrogenic Differentiation Capacity of Progeroid *Zmpste24*$^{-/-}$ MDSPCs

MDSPC pellet cultures were cultivated with or without rapamycin and maintained for 14 days prior to staining with Alcian Blue, a well-known chondrogenic stain. Chondrogenic differentiation was significantly impaired in the *Zmpste24*$^{-/-}$ MDSPCs compared to the WT MDSPCs ($p < 0.001$; Figures 6A–6C). The impaired differentiation of the progeroid MDSPCs was significantly improved with rapamycin treatment ($p < 0.05$; Figures 6A–6C). This finding was also confirmed via qPCR of two chondrogenic markers: type II

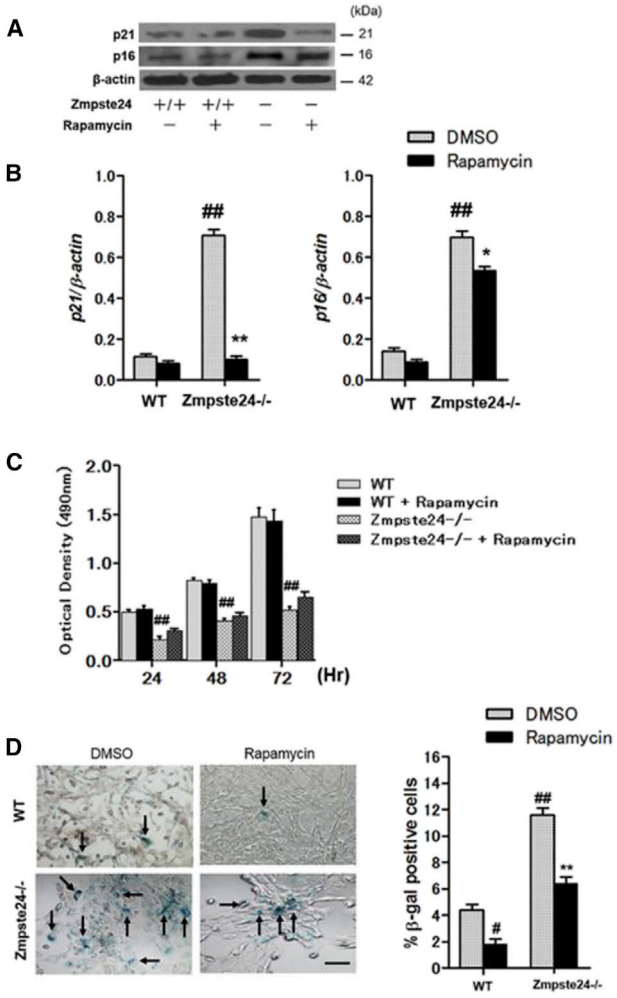

Figure 4. Rapamycin's Effect on Senescence Markers in *Zmpste24*$^{-/-}$ MDSPCs

(A) Representative western blots showing expression of senescence-related markers p21 and p16 in MDSPCs isolated from *Zmpste24*$^{-/-}$ and WT mice, cultured with and without rapamycin. (B) Quantification p21 and p16 expression relative to β-actin (n = 4; ##p < 0.001 versus WT DMSO; **p < 0.001 versus *Zmpste24*$^{-/-}$ DMSO; *p < 0.05 versus *Zmpste24*$^{-/-}$ DMSO). (C) Proliferation of *Zmpste24*$^{-/-}$ and WT MDSPCs, with or without rapamycin expressed as optical density (490 nm). (D) Representative images of SA-β-gal assay for labeling senescence of MDSPCs isolated from *Zmpste24*$^{-/-}$ and WT mice, cultured with and without rapamycin. Scale, 50 μm. Arrow, SA-β-gal-positive (blue) cells. Percentage of SA-β-gal-positive cells from four independent MDSPC populations (#p < 0.05, ##p < 0.001 versus WT DMSO; **p < 0.001 versus *Zmpste24*$^{-/-}$ DMSO).

collagen alpha 1 (*Col2A1*) and *aggrecan* (Figures 6D and 6E). Expression levels of *Col2A1* and *aggrecan* were significantly reduced compared to those in the WT MDSPCs (*Col2A1*, p < 0.001; *aggrecan*, p < 0.001). However, expression levels of *Col2A1* and *aggrecan* were significantly increased in the *Zmpste24*$^{-/-}$ MDSPCs after rapamycin treatment (*Col2A1*, p < 0.05; *aggrecan*, p < 0.001), demonstrating that mTORC1 inhibition improves chondrogenic differentiation of *Zmpste24*$^{-/-}$ MDSPCs.

Zmpste24$^{-/-}$ MDSPCs Have Reduced Osteogenic Capacity That Is Largely Unaffected by Rapamycin Treatment

Alizarin Red staining, an established staining technique that detects calcific depositions of osteogenic origins, was performed in *Zmpste24*$^{-/-}$ MDSPCs and WT MDSPCs cultivated in monolayer cultures with osteogenic medium, with or without rapamycin treatment. Following osteogenic induction, WT MDSPCs exhibited a significantly higher concentration of Alizarin Red staining, indicating increased osteogenic differentiation capacity, compared to the *Zmpste24*$^{-/-}$ MDSPCs (p < 0.05; Figures 7A and 7B). However, the impaired differentiation capacity of the progeroid MDSPCs was not significantly improved after rapamycin treatment (p = 0.072; Figures 7A and 7B). The effect of rapamycin treatment on the defective osteogenic differentiation pathway was further assessed through measurement of the mRNA expression levels of two osteogenic markers: type I collagen alpha 1 (*Col1A1*) and *osteocalcin*. The expression levels of *Col1A1* and *osteocalcin* in MDSPCs isolated from the progeroid mice were significantly reduced compared to the WT MDSPCs (*Col1A1*, p < 0.001; *osteocalcin*, p < 0.05; Figures 7C and 7D). However, the expression level of *osteocalcin*, but not that of *Col1A1*, was significantly increased in the *Zmpste24*$^{-/-}$ MDSPCs after rapamycin treatment (*Col1A1*, p = 0.734; *osteocalcin*, p < 0.05; Figures 7C and 7D). These data highlight reduced osteogenic potential in *Zmpste24*$^{-/-}$ MDSPCs, and rapamycin increased the osteocalcin expression of the *Zmpste24*$^{-/-}$ MDSPCs.

Rapamycin Reduces the Adipogenic Differentiation Capacity of Progeroid *Zmpste24*$^{-/-}$ MDSPCs

A disruption of the adipo-osteogenic axis toward adipogenesis during aging is thought to contribute to age-associated obesity, osteopenia, and osteoporosis.[34] Furthermore, mTORC1 signaling is a fundamental contributor to the process of adipogenesis.[35] To examine the role of mTORC1 in the adipogenic program in progeroid cells, *Zmpste24*$^{-/-}$ MDSPCs were cultured in adipogenic medium for 15 days, with or without rapamycin, and then stained using the lipid stain Oil Red O. The adipogenic differentiation capacity was significantly enhanced in the *Zmpste24*$^{-/-}$ MDSPCs compared to the WT MDSPCs (p < 0.001; Figures 8A and 8B). In addition, adipogenic differentiation in the progeroid MDSPCs was significantly attenuated after rapamycin treatment (p < 0.05; Figures 8A and 8B). Levels of mRNA for two adipogenic markers, peroxisome proliferator-activated receptor gamma (*PPARγ*) and lipoprotein lipase (*LPL*), were also measured. The expression levels of both *PPARγ* and *LPL* were significantly increased in the progeroid MDSPCs compared to the WT MDSPCs (p < 0.001; Figure 8C and 8D). Interestingly, *Zmpste24*$^{-/-}$ MDSPCs treated with rapamycin exhibited significantly reduced levels of both *PPARγ* and *LPL* expression relative to *Zmpste24*$^{-/-}$ MDSPCs without rapamycin treatment (*PPARγ*, p < 0.001; *LPL*, p < 0.05; Figure 8C and 8D). Overall, these data indicate an increase in the adipogenic signaling program in *Zmpste24*$^{-/-}$ MDSPCs, compared to WT MDSPCs, that is at least partially regulated by reducing the mTORC1 activity.

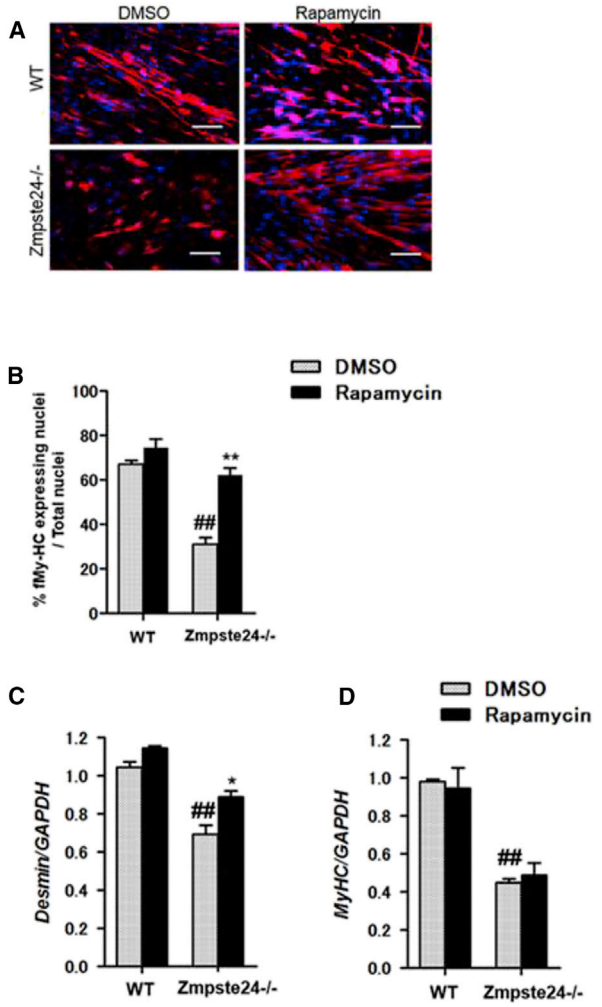

Figure 5. Myogenic Differentiation Potential of MDSPCs Isolated from Progeroid *Zmpste24*$^{-/-}$ Mice

(A) Representative images of *in vitro* myogenic differentiation of MDSPCs isolated from *Zmpste24*$^{-/-}$ and WT mice, cultured with and without rapamycin. Cells were immunostained for the terminal differentiation marker f-My-HC (red) and counterstained with DAPI for visualizing nuclei (blue). Original magnification, ×200. Scale bar, 50 μm. (B) Quantification of myogenic differentiation was calculated as the fraction of cells (DAPI, blue) expressing f-My-HC (red) from four independent MDSPC populations ($p < 0.001$ versus WT DMSO; **$p < 0.001$ versus *Zmpste24*$^{-/-}$ DMSO). (C and D) qPCR results indicating mRNA expression levels of terminal myogenic differentiation markers, *desmin* (C) and *MyHC* (D), after myogenic differentiation of MDSPCs isolated from *Zmpste24*$^{-/-}$ and WT mice, cultured with and without rapamycin treatment (n = 4; ##$p < 0.001$ versus WT DMSO; *$p < 0.05$ versus *Zmpste24*$^{-/-}$ DMSO).

DISCUSSION

mTORC1 regulates cellular processes, such as protein synthesis in response to energy needs and oxidative stress.[36,37] Numerous studies have implicated mTORC1 signaling in systemic aging and stem function.[27,28,38,39] The results of the current study demonstrate that rapamycin treatment can reduce the upregulated mTORC1 activity in *Zmpste24*$^{-/-}$ MDSPCs. We also show that reducing mTORC1 activity reduced the level of senescence markers and improved function of the progeroid cells by increasing the capacity for myogenic and chondrogenic differentiation with a decreased trend toward adipogenic differentiation. This observation is consistent with the possibility that nuclear abnormalities causing premature aging in *Zmspte24*-null mice trigger downregulation of differentiation and initiation of stress responses and pathophysiologies associated with the development of progeroid symptoms. Indeed, several studies demonstrated that nuclear envelope abnormalities accelerate aging and may also contribute to the process of normal aging.[40,41] This supports the concept that genetically engineered progeroid models can be useful, not only in studying mechanisms that underlie the processes involved with normal aging, but also in evaluating potential therapeutic treatments.[3] Accordingly, we recently used naturally aged mice and excision repair cross-complementation group-1 *Ercc1*$^{-/\Delta}$ mice (a mouse model of XFE progeria) and demonstrated that MDSPCs isolated from both progeria models had a loss of "stemness," including the loss of proliferation and multi-lineage differentiation capacities.[17,28] Given *Ercc1*$^{-/\Delta}$ mice exhibit progeria via a completely different mechanism, there may thus be a fundamental role for mTORC1 signaling in MDSPCs during the aging process.

Apoptosis and senescence are well-documented cellular responses to DNA damage.[42,43] In the present study, we demonstrated that MDSPCs isolated from progeroid *Zmpste24*$^{-/-}$ mice have a greater tendency toward apoptosis and cellular senescence when compared to WT MDSPCs, which corroborates the results reported in previous studies.[44–46] Several previous studies have also found that rapamycin can decelerate cellular senescence, especially in stem cells.[47–50] In agreement, we found that rapamycin decreased several markers of senescence, leading to functional improvement of the progeroid *Zmpste24*$^{-/-}$ MDSPCs. Future studies will examine if these effects are due to a reduction in stress signaling pathways, altered autophagic flux, or apoptosis-related protein expression directly. Nonetheless, the decreased capacity for myogenic and chondrogenic differentiation of MDSPCs isolated from *Zmpste24*$^{-/-}$ mice seems to be related to the increased levels of apoptosis and cellular senescence observed.[51]

The most striking pathologic phenotype of *Zmpste24*$^{-/-}$ mice is most likely the significant musculoskeletal pathologies, such as muscle atrophy, osteopenia, and osteoporosis resulting in spontaneous bone fractures, akin to those occurring in mouse models of osteogenesis imperfecta.[29] It is known that mutations of the lamin A gene, a major structural component of the nuclear envelope, have negative impacts on skeletal muscle function and myoblast differentiation.[6,9,10,29,52,53] Ramos et al.[27] reported that mTORC1 signaling is hyper-activated in both skeletal and cardiac muscle in *Lmna*$^{-/-}$ mice. Rapamycin also decreased mTORC1 signaling, improved skeletal and cardiac muscle function, and increased the lifespan of these mice.[27] Furthermore, human mesenchymal stem cells (hMSCs) isolated from HGPS patients exhibit defective lamin A processing.[54] We also found that MDSPCs isolated from *Zmpste24*$^{-/-}$ had nuclear lamin A abnormalities concomitant with decreased myogenic potential, a finding that we similarly found in the *Ercc1*$^{-/\Delta}$ progeria mice.[28] It should be noted

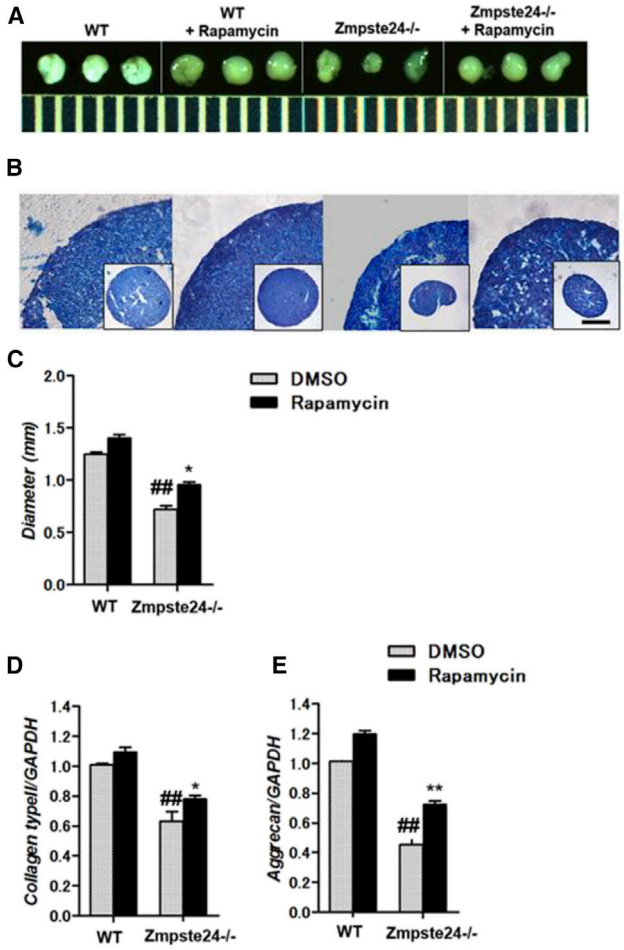

Figure 6. Chondrogenic Differentiation Potential of MDSPCs Isolated from Progeroid *Zmpste24*$^{-/-}$ Mice

(A) Representative images of *in vitro* chondrogenic pellets (ruler is in mm) from MDSPCs isolated from *Zmpste24*$^{-/-}$ and WT mice, cultured with and without rapamycin. (B) Representative images of Alcian Blue staining of each pellet (blue, chondrogenesis). Scale bar, 500 μm. Original magnification, ×200, ×40 in inset. (C) Measurement of diameter of chondrogenic pellets (##$p < 0.001$ versus WT DMSO; *$p < 0.05$ versus *Zmpste24*$^{-/-}$ DMSO). (D and E) qPCR results indicating mRNA expression levels of the chondrogenic differentiation markers, *Col2a1* (D) and *aggrecan* (E), after chondrogenic differentiation of MDSPCs isolated from *Zmpste24*$^{-/-}$ and WT mice, cultured with and without rapamycin treatment (n = 4; ##$p < 0.001$ versus WT DMSO; *$p < 0.05$, **$p < 0.001$ versus *Zmpste24*$^{-/-}$ DMSO).

that skeletal muscle tissues are highly adaptable and that many signaling pathways regulate muscle remodeling. Recent studies have indicated that the formation of skeletal muscle is a tightly regulated process that is critically modulated by Wnt signaling. Myogenesis is dependent on the precise and dynamic integration of multiple Wnt signals, allowing self-renewal and the progression of muscle precursors along the myogenic lineage.[55] In addition, it remains unclear whether defects in MDSPC function arise because of defects in the stem cells, stem cell niche, or both.[56] Therefore, future studies are needed to investigate the dynamic mechanisms that underlie MDSPC dysfunction within the skeletal muscle niche during the process of aging.

Cortical and trabecular bone volumes also are significantly reduced in *Zmpste24*$^{-/-}$ mice.[29] We therefore hypothesized that the osteogenic potential of stem cells from *Zmpste24*$^{-/-}$ mice might be reduced, and indeed found that the osteogenic differentiation capacity of *Zmpste24*$^{-/-}$ MDSPCs was significantly reduced when compared to WT MDSPCs. However, the impaired osteogenic differentiation capacity of the progeroid MDSPCs was not significantly improved after rapamycin treatment, despite the increase in osteocalcin expression. Although it is still unclear why rapamycin does not improve the osteogenic potential of progeroid MDSPCs, there is evidence indicating rapamycin's inhibitory effect on VEGF-mediated signaling, an important feature for osteogenesis and bone repair.[57–59] Furthermore, it has been reported that rapamycin inhibits VEGF-induced microvascular hyperpermeability and VEGF-A^{164}-driven angiogenesis.[60] Although osteogenic differentiation was seemingly unaffected by rapamycin, we did find that rapamycin treatment improved the myogenic and chondrogenic differentiation capacities of *Zmpste24*$^{-/-}$ MDSPCs. These observations suggest that abnormally increased activation of the mTORC1 pathway may be involved in stem cell depletion/exhaustion, which is also linked to an accelerated aging phenotype.[28] Downstream factors in the mTORC1 pathway, including 4E-BP1, bind to mRNA and regulate translation, thereby controlling the rates of protein synthesis and cell growth.[61–63] Indeed, we observed elevated p4E-BP1 in *Zmpste24*$^{-/-}$ MDSPCs that was significantly reduced with rapamycin treatment. Of note, the effects of rapamycin were reduced in WT MDSPCs, very likely because of the lower activity of mTORC1 in WT cells.

It has been shown that hematopoietic stem cells (HSCs) from naturally aged mice have elevated mTORC1 activity, and increasing mTORC1 signaling in young mice induces premature aging.[44] Along these lines, rapamycin delays cellular senescence and aging, abrogates nuclear blebbing, and stimulates the degradation of progerin in HGPS cells[64,65] through a mechanism that probably involves the stimulation of autophagic degradation.[66] Moreover, it was reported that activation of the autophagic pathway using rapamycin can counteract progerin and farnesylated prelamin A accumulation in HGPS cells.[67] Thus, rapamycin partially attenuates defective lamin A processing and represents a potential therapeutic option for HGPS patients. However, rapamycin does have reported side effects, such as elevated serum cholesterol and triglycerides, anemia, proteinuria, skin rashes, diarrhea, immunosuppressive effects, and delayed wound healing,[68,69] which may be exacerbated in frail patients with HGPS. Lynch[70] also found that leucine, an α-amino acid, regulates mTORC1 signaling in adipocytes and some other cells. Further studies are needed for investigating alternatives to rapamycin, including rapamycin analogs, with respect to rescuing age-related changes in MDSPCs. Indeed, second-generation mTOR inhibitors that act as ATP-competitive mTOR kinase inhibitors that can block mTORC1 and -2, and other upstream mTOR regulators have been developed[71] and shown to be more potent than rapamycin and can reduce protein translation,

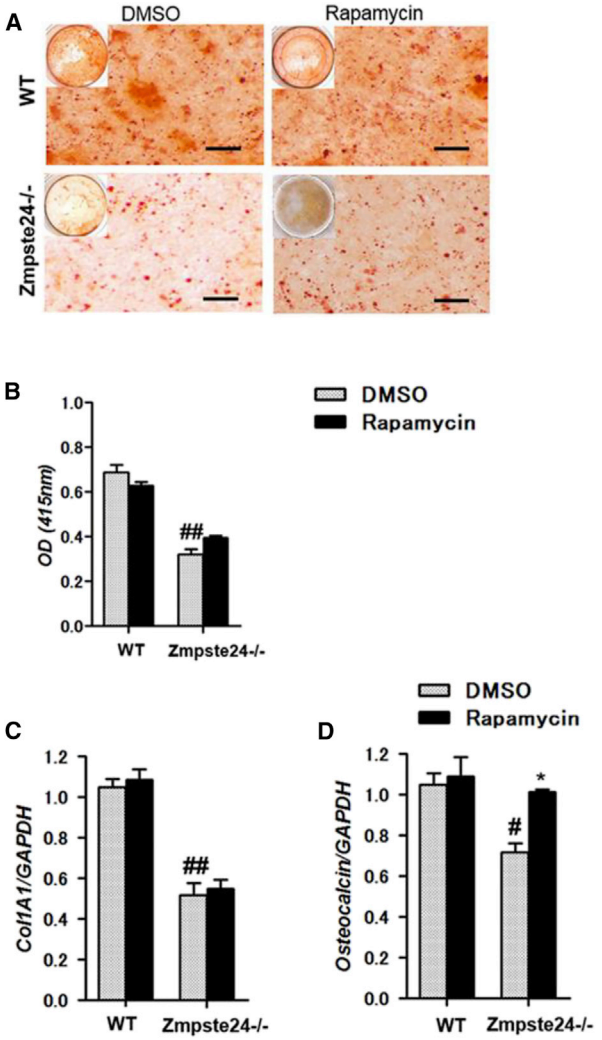

Figure 7. Osteogenic Differentiation Potential of MDSPCs Isolated from Progeroid *Zmpste2*$^{-/-}$ Mice

(A) Representative images of *in vitro* Alizarin Red staining of MDSPCs isolated from *Zmpste24*$^{-/-}$ and WT mice, cultured with and without rapamycin. Left upper panels in each image represent whole images. Scale bar, 50 μm. (B) Quantification of alizarin red staining by photometric analysis. The extracted alizarin red dye was measured with an absorption spectrometer at 415 nm wavelength. The amount of alizarin red dye was expressed as an optical density (#$p < 0.05$ versus WT DMSO). (C and D) qPCR results indicating mRNA expression levels of osteogenic differentiation markers, *Col1A1* (C) and *osteocalcin* (D), after osteogenic differentiation of MDSPCs isolated from *Zmpste24*$^{-/-}$ and WT mice, cultured with and without rapamycin treatment (n = 4; #$p < 0.05$, ##$p < 0.001$ versus WT DMSO; *$p < 0.05$ versus *Zmpste24*$^{-/-}$ DMSO).

attenuate cell cycle progression, and inhibit angiogenesis in many cancer cells. The advent of these agents will allow for the identification of specific subunit(s) of mTOR that exert pivotal roles in progeria. However, the aim of this study was to use rapamycin as a tool to inhibit mTORC1 to determine its role in differentiation and senescence of progeroid MDSPCs. Further studies *in vivo* are needed to examine the effects of rapamycin, or *rapalogs*, on endogenous MDSPCs and other stem cell populations on health and function in the context of progeria or natural aging. Nonetheless, the promising perspectives raised by these results and recent reports[27,67] highlight mTORC1 signaling and the potential applications of mTORC1 inhibitors to counteract age-associated diseases and consequently increase longevity.

In summary, our findings indicated that hyper-activation of the mTORC1 in *Zmpste24*$^{-/-}$ MDSPCs contributed to their dysfunction. Through the inhibition of mTORC1, rapamycin was capable of significantly improving the differentiation capacity while attenuating senescence and apoptosis of progeroid MDSPCs. The role of mTORC1 and its inhibition by rapamycin has been shown to modulate oxidative stress response genes in several studies *in vitro* and *in vivo*. Thus, it is likely that a reduction in oxidative stress via the induction of various antioxidant genes, a response noted in several studies,[72,73] may have played a role in the improved health and function of MDSPCs here. The results of this study provide additional insight into the spontaneous and premature onset of age-related degenerative changes associated with progeroid syndromes and the role that mTORC1 signaling has in the age- related dysfunction of adult stem cells.

MATERIALS AND METHODS

Mice

Zmpste24$^{-/-}$ mouse genotyping was performed via PCR.[8] All animal experiments were performed in accordance with the Institutional Animal Care and Use Committee of the University of Pittsburgh. Mice were originally developed on a mixed background of 50% C57BL/6 and 50% 129 SvJae. Here, *Zmpste24*$^{-/-}$ mice were generated by crossing heterozygous animals, and *Zmpste24*$^{+/+}$ littermates were used as controls or WT.

Skeletal Preparation and Micro-CT

Two-day- and 8-week-old *Zmpste24*$^{-/-}$ mice and WT mice were skinned, eviscerated, and fixed in 95% ethanol. Alcian Blue staining was performed, followed by placement into potassium hydroxide to remove the soft tissue. After the cartilage was stained and visualized, Alizarin Red staining was performed to evaluate overall skeletal properties.[74] We also used micro-CT (high-resolution scanner vivaCT 40; Scanco Medical, Brüttisellen, Switzerland) for microarchitectural analysis. Parameters used for the scans were as follows: tube voltage, 50 kVp; tube current, 160 μA; integration time, 3.6 ms; and axial field of view, 48 mm, with an isotropic voxel size of 10 μm.

Isolation of MDSPCs

MDSPCs were isolated from the hindlimb skeletal muscles of 8-week-old (age-matched) WT, 8-week-old (age-matched) progeroid *Zmpste24*$^{-/-}$, and aged (24-month-old) WT (n = 4 per strain, all male) mice using a previously described modified preplating technique.[11,12] MDSPCs were cultured in proliferation medium (PM) containing high-glucose DMEM, supplemented with 10% fetal bovine serum (FBS), 10% horse serum, 1% penicillin/streptomycin (all from

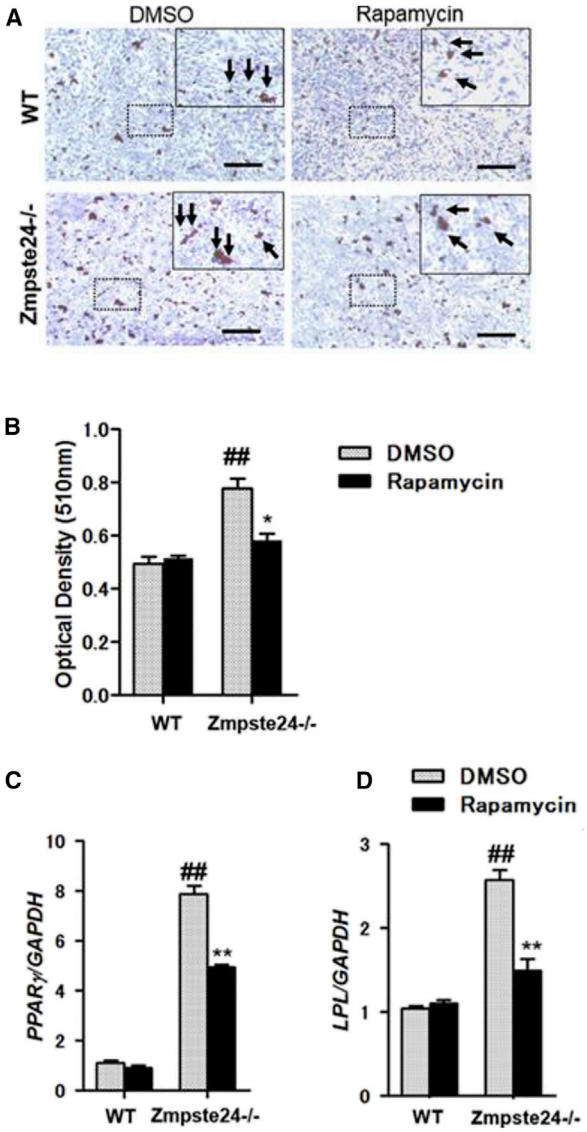

Figure 8. Adipogenic Differentiation Potential of MDSPCs Isolated from Progeroid *Zmpste24*$^{-/-}$ Mice

(A) Representative images of Oil Red O (lipid) staining of MDSPCs isolated from *Zmpste24*$^{-/-}$ and WT mice, cultured with and without rapamycin. Right upper panels in each image indicate high magnification of the area surrounded by a dotted square. Arrows indicate positive Oil Red O staining. Scale bar, 50 μm. (B) Quantification of Oil Red O staining by photometric analysis. Absorbance of Oil Red O was measured at a wavelength of 510 nm (##$p < 0.001$ versus WT DMSO; *$p < 0.05$ versus *Zmpste24*$^{-/-}$ DMSO). (C and D) qPCR results indicating mRNA expression levels of adipogenic differentiation markers, *PPARγ* (C) and *LPL* (D), after adipogenic differentiation of MDSPCs isolated from *Zmpste24*$^{-/-}$ and WT mice, cultured with and without rapamycin treatment (n = 4; ##$p < 0.001$ versus WT DMSO; **$p < 0.001$ versus *Zmpste24*$^{-/-}$DMSO).

Invitrogen, Grand Island, NY, USA), and 0.5% chick embryo extract (Accurate Chemical, Westbury, NY, USA), within flasks coated with type I collagen (Sigma-Aldrich, St. Louis, MO, USA) at a density of 3×10^5 cells per well in PM. At 70% confluence, the cells were dissociated with trypsin/EDTA, replated at a cell density of 1.0–2.5 $\times$ 10^3 cells/cm^2, and cultured for 3–4 weeks before performing the below-described cell treatments. All cells used in this study, except for cells examined with long-term culturing conditions (described below), were passaged <10 times.

Rapamycin Treatments

Rapamycin was obtained from LC Laboratories (Woburn, MA, USA), dissolved in dimethylsulfoxide (DMSO) at 50 mg/mL, and stored at −20°C. *Zmpste24*$^{-/-}$ and WT MDSPCs were treated with 10 nM rapamycin to inhibit mTORC1. As a control, the same amount of DMSO was used to treat MDSPCs from these two populations. A concentration of 10 nM rapamycin was selected, because this concentration is effective in improving myogenic differentiation without inducing cellular toxicity.[28] To evaluate the effects of rapamycin on MDSPCs, we established four groups: WT MDSPCs, WT MDSPCs+rapamycin, *Zmpste24*$^{-/-}$ MDSPCs, and *Zmpste24*$^{-/-}$ MDSPCs+rapamycin. We carefully chose the rapamycin concentration to avoid severe side effects, based on our previous work, and used normal PM, not reduced or serum-free medium.[28]

Western Blot Analysis

Protein extraction was performed 24 h after rapamycin treatment. MDSPCs from WT and *Zmpste24*$^{-/-}$ mice were lysed in radioimmunoprecipitation assay (RIPA) buffer (Sigma-Aldrich) and Laemmli Sample Buffer (Bio-Rad, Hercules, CA, USA), boiled for 5 min, and centrifuged for 5 min at 3,000 $\times$ *g*. Protein concentrations were measured by using Bradford protein assay reagent (Bio-Rad). A total of 15 μg of protein from each sample was loaded on 10% SDS-polyacrylamide gels then transferred to PVDF membranes (Millipore, Billerica, MA, USA). Membranes were blocked with 5% nonfat dry milk (Bio-Rad, Hercules, CA, USA) in Tris-buffered saline Tween-20 (TBST) then incubated overnight at 4°C with primary antibodies. Membranes were then probed with horseradish-peroxidase (HRP)-conjugated secondary antibodies at room temperature. Proteins were visualized with SuperSignal West Femto, using enhanced chemiluminescent substrate (Thermo Scientific, Rockford, IL, USA), and the chemical luminescence reaction was visualized with a FOTO/Analyst Luminary/Fx CCD imaging system (Fotodyne Inc., Hartland, WI, USA). The following primary antibodies were used in this study: rabbit anti-FACE-1 (Zmpste24; sc-66886, 1:200), goat anti-prelamin A C-terminal (sc-6214, 1:200), rabbit anti-β-actin (sc-4970, 1:5,000; Santa Cruz Biotechnology, Santa Cruz, CA); mouse anti-vinculin (1:2,000, V4505; Sigma-Aldrich, St. Louis, MO USA); rabbit anti-mTORC1 (1:200, 2942), rabbit anti-phospho-mTORC1 (p-mTORC1; 5536, 1:200), rabbit anti-phospho-eukaryotic translation initiation factor 4 (eIF4)-E binding protein 1 (p-4E-BP1; Thr37/46; 2855, 1:200), rabbit anti-eIF4E binding protein 1 (4E-BP1; 9452, 1:200), rabbit anti-phospho-AMP-activated protein kinase (p-AMPK; 2535, 1:200), rabbit anti-AMPK (2532, 1:200), rabbit anti-phospho-AKT (p-AKT; 9271, 1:200), rabbit anti-AKT (AKT; 9272, 1:200), rabbit anti-PARP (9542, 1:200), rabbit anti-p16 (4824, 1:200), and rabbit anti-p21 (1:200; Cell Signaling Technology,

Beverly, MA). Secondary antibodies used were HRP-conjugated goat anti-rabbit IgG (7074, 1:10,000; Cell Signaling Technology), and HRP-conjugated donkey anti-goat IgG (sc-2020, 1:10,000, Santa Cruz Biotechnology). The density of each blot was quantified by using ImageJ (NIH) normalized to β-actin or vinculin and each blot was representative of four biological replicates.

Immunohistochemical Staining

Fibrosis in skeletal muscle (gastrocnemius) cryosections was determined by using Masson's trichrome staining to detect the collagen I content according to the manufacturer's protocol (Masson's Trichrome stain kit; IMEB, Inc., San Marcos, CA, USA). Images of the histological samples were obtained with a Nikon Eclipse E800 microscope. To detect abnormal cell nuclei, immunohistochemistry was performed. Cultured cells were fixed in 4% paraformaldehyde and permeabilized with 0.2% Triton X-100 (Sigma-Aldrich, St. Louis, MO, USA). The cells were then incubated with Block Ace Solution (Dako Japan, Kyoto, Japan) and stained with antibodies against lamin A/C (1:50; Santa Cruz Biotechnology) as a sensitive marker for the nuclear lamina, followed by incubation for 1 h with an Alexa Fluor 594-conjugated rabbit anti-goat IgG_1 (1:1,000; Molecular Probes, Grand Island, NY, USA). The nuclei were counterstained with DAPI solution (1:500; Sigma-Aldrich) for 5 min, in order to visualize the nuclei. The morphological definition of abnormal nuclei is the presence of more than two lobulations at the surface.[5] Images were obtained with a Leica DM IRB microscope equipped with a Retiga digital camera and were evaluated with Northern Eclipse software (v6.0; Empix Imaging). Cells were quantified using ImageJ (NIH) image-analysis software, and results are expressed as the percentage of cells with abnormal nuclei per region of interest (ROI).

Apoptosis Detection

Apoptotic cell death was evaluated in cultured cells using the *In Situ* Cell Death Detection Kit containing fluorescein (Roche Applied Science, Philadelphia, PA, USA) for TUNEL detection, according to the manufacturer's protocol. To visualize the nuclei, the cultures were incubated with DAPI for 10 min. The number of cells that were TUNEL positive was calculated and averaged across 15 fields, each from three replicate cell culture plates in four independent experiments. The percent of apoptotic cells was calculated as TUNEL-positive cells divided by the total number of cells (×100). Images were obtained and evaluated using the same equipment and analysis tools, as mentioned above.

Cellular Senescence Assay

Cellular senescence was evaluated in cultured cells using the Senescence β-Galactosidase Staining Kit (Cell Signaling Technology) for senescence-associated β-galactosidase (SA-β-gal) activity, according to the manufacturer's protocol. The number of cells that were SA-β-gal positive was calculated and averaged across 15 fields, each from three replicate plates in four independent experiments. The percentage of senescent cells was calculated as SA-β-gal-positive cells divided by the total number of cells and then multiplied by 100. Images were obtained and evaluated using the same equipment and analysis tools as mentioned above.

Proliferation Assays

MDSPCs were seeded onto 96-well culture plates at a density of 5×10^3 cells per well and cultured in endothelial cell basal medium (EBM2) with 10% FBS for three separate time points during the experiment (24, 48, and 72 h) at 37°C in 20% O_2 and 5% CO_2. Optical density was measured on a plate reader at 490 nm wavelength. The proliferation activities of *Zmpste24*$^{-/-}$ mice and WT mice-derived MDSPCs were examined using the colorimetric Cell Counting Kit (CCK-8; Dojindo Laboratories, Kumamoto, Japan), whereby a formazan dye signal is directly proportional to the viable number of cells. This protocol is an established method of detecting and tracking live cells, as previously described.[75]

Myogenic Differentiation Assay

MDSPCs were seeded onto collagen-type-I-coated six-well plates (1×10^5 cells/well) and cultured for 3 days in PM. Myogenic differentiation was induced by replacing the PM with differentiation medium (DMEM, 2% FBS, and 1% penicillin/streptomycin) and cultured for 4 days, as previously described,[19] with or without 10 nM rapamycin. On day 7, immunostaining for f-MyHC, a marker of terminal myogenic differentiation, was performed, to stain for differentiated muscle cells. Cells were fixed with methanol, blocked with 5% goat serum, and incubated at room temperature with primary mouse anti-MyHC fast (1:250; Sigma-Aldrich) and secondary biotinylated IgG (1:250; Vector Laboratories, Burlingame, CA, USA) for 1 h each. The cells were then incubated in the same conditions for an additional 15 min, following the addition of streptavidin-594 (1:500; Sigma-Aldrich) which was used to fluorescently label the myotubes. The nuclei were then visualized by staining with DAPI for 10 min. Myogenic differentiation was calculated as the percentage of cells expressing f-MyHC. Total cell nuclei and nuclei within f-MyHC-positive myofibers, from 15 fields, each from three replicate plates, were counted using ImageJ. Total RNA was extracted as described below for qRT-PCR analysis. Myogenic gene expression of *MyHC* and *desmin* was analyzed. Images were obtained and evaluated using the same equipment and analysis tools as mentioned above.

Chondrogenic Differentiation Assessment

Pellet culture was performed as described previously.[76] Pellets were made in 0.5 mL of chondrogenic medium (Lonza, Allendale, NJ, USA) supplemented with 10 ng/mL transforming growth factor-β3 (TGF-β3; R&D System, Minneapolis, MN, USA), with or without 10 nM rapamycin. The pellets were incubated at 37°C in 5% CO_2 and the medium was changed every 3 days. Pellets were harvested after 14 days in culture. Cultured micromass pellets were fixed with 10% neutral-buffered formalin containing 0.1% cetylpyridinium chloride. The longest and shortest diameters of the pellets were measured using ImageJ software (NIH). Average diameters of the pellets were obtained by dividing the sum of diameters measured for each pellet by the number of measurements.[77,78] Pellets were stained with 1% Alcian Blue (pH 1.0) for 30 min in order to stain the highly sulfated

proteoglycans that are characteristic of cartilaginous matrices. Data from three replicate plates for four independent experiments were analyzed. Total RNA was extracted for qRT-PCR analysis. The expression patterns of chondrogenic genes expressing collagen type 2A1 (*Col2A1*) and *aggrecan* were analyzed.

Osteogenic Differentiation Assessment

Osteogenic differentiation assays were performed as previously reported[79] in non-collagen coated flasks. Briefly, 100,000 cells were plated in 6-well plates and cultured under specific osteogenic conditions in DMEM supplemented with 10% FBS (Sigma-Aldrich), 100 U/mL penicillin/streptomycin solution (Sigma-Aldrich), 0.1 mM dexamethasone (Sigma-Aldrich), 50 μM ascorbate-2-phosphate (Sigma-Aldrich), 10 mM β-glycerophosphate (Sigma-Aldrich), and 100 ng/mL bone morphogenetic protein-2 (BMP2; Medtronic), with or without 10 nM rapamycin, and incubated at 37°C in 5% CO_2. Mineralization was assessed by Alizarin Red staining on day 21. The cultures were rinsed twice with PBS, fixed in 100% ethanol for 30 min, and stained with 1% Alizarin Red (Hartman Leddon, Philadelphia, PA, USA) in 0.28% ammonia water for 10 min at room temperature. The stained cell layers were washed twice with distilled water and air dried for micro-/macroscopic analyses. For quantification, Alizarin Red dye was extracted from the stained cell layer with 5% formic acid solution, and the optical density was measured with a photometer (microplate reader Model 680; Bio-Rad, Tokyo, Japan) at a 415 nm wavelength. Total RNA was extracted for qRT-PCR analysis. The expression patterns of osteogenic genes expressing collagen type 1 alpha 1 (*Col1A1*) and *osteocalcin* were analyzed.

Adipogenic Differentiation Assessment

MDSPCs were seeded in 12-well plates at a concentration of 1×10^5 cells per well. After the cells had reached confluence, adipogenic differentiation was induced by exposure to three cycles of standard induction/maintenance media, with or without 10 nM rapamycin. This consisted of culturing the cells for 72 h in adipogenic induction medium containing dexamethasone, 3-isobutyl-1-methyl-xanthine (IBMX), recombinant human insulin, and indomethacin, followed by 48 h of culture in maintenance medium (Lonza). To detect adipogenic differentiation, Oil Red O staining was performed. Lipid droplets in the cells exposed to adipogenic medium were stained with 1-([4-(xylylazo)xylyl]azo)-2-naphthol (Oil Red O; Sigma). Cells were fixed in 4% neutral-buffered formalin overnight at 4°C and then washed with 60% isopropanol (500 μL) on a shaker for 30 min. Oil Red O was dissolved in isopropanol (175 mg/50 mL), diluted in PBS to create a 60% working solution, and filtered through a 0.45 μm syringe filter. The isopropanol wash was aspirated from the wells, the Oil Red O solution was added (200 μL), and the cells were placed on a shaker for 30 min. The dye solution was then aspirated, and the wells were washed with PBS (500 μL) four times over the course of 1 h. Finally, the cells were counterstained with hematoxylin and imaged with a light microscope. For quantification, Oil Red O staining was solubilized in isopropanol, and the absorbance was measured at a wavelength of 510 nm, as previously described.[80] Data obtained from three replicate plates for four independent experiments were analyzed. Total RNA was extracted for qRT-PCR analysis. Adipogenic gene expression of peroxisome *PPARγ* and *LPL* were analyzed.

RNA Isolation and Real-Time qPCR

Total RNA was obtained from cultured cells using an RNeasy Mini Kit (QIAGEN, Hilden, Germany) according to the manufacturer's protocol. One microgram total RNA was used for random-hexamer-primed cDNA synthesis with the SuperScript II pre-amplification system (Invitrogen). qRT-PCR reactions were performed in triplicate using iQ5 (Bio-Rad) and Maxima SYBR Green/ROX qRT-PCR Master Mix (Thermo Fisher Scientific), along with gene-specific primers. The primers were designed according to the sequences obtained from the GenBank database (Supplementary Table 1). Melting curve analysis was performed with Dissociation Curves Software (Applied Biosystems, Waltham, MA, USA). Results were obtained using sequence detection software (StepOne Software v2.3) and the mean cycle threshold (Ct) values were used to calculate gene expression normalized to that of mouse glyceraldehyde-3-phosphate dehydrogenase (GAPDH).

Statistical Analyses

The results were analyzed with a statistical software package (GraphPad Prism, MDF Software, La Jolla, CA). All values were expressed as mean ± SEM. Multiple comparisons among groups were made using one-way ANOVA followed by *post hoc* testing using Tukey's procedure. A value of $p < 0.05$ was considered to be statistically significant.

SUPPLEMENTAL INFORMATION

Supplemental Information can be found online at https://doi.org/10.1016/j.omtm.2019.05.011.

AUTHOR CONTRIBUTIONS

The concept, experimental design, and funding support of this project were provided by J.H., L.J.N., P.D.R., and F.H.F. Experiments and data analyses were performed by Y.K., K.T., A.L., J.H.C., J.T., X.M., T.M., Y.T., R.K., and M.K. Scientific consultation, experimental design, and writing were performed by Y.K., W.S.H., and J.H.

CONFLICT OF INTEREST

J.H. receives royalties from Cook Myosite, Inc. The remaining authors declare no competing interests.

ACKNOWLEDGMENTS

The authors are grateful for the scientific advice and editorial assistance of Lavanya Rajagopalan and Mary Hall. The work was supported by start-up funding from University of Texas Health Science Center at Houston and the Steadman Philippon Research Institute, as well as NIH grant NIA P01 AG043376.

REFERENCES

1. Kirkwood, T.B. (2005). Understanding the odd science of aging. Cell *120*, 437–447.
2. Vijg, J. (2008). The role of DNA damage and repair in aging: new approaches to an old problem. Mech. Ageing Dev. *129*, 498–502.

3. Hasty, P., Campisi, J., Hoeijmakers, J., van Steeg, H., and Vijg, J. (2003). Aging and genome maintenance: lessons from the mouse? Science *299*, 1355–1359.

4. Sullivan, T., Escalante-Alcalde, D., Bhatt, H., Anver, M., Bhat, N., Nagashima, K., Stewart, C.L., and Burke, B. (1999). Loss of A-type lamin expression compromises nuclear envelope integrity leading to muscular dystrophy. J. Cell Biol. *147*, 913–920.

5. Goldman, R.D., Shumaker, D.K., Erdos, M.R., Eriksson, M., Goldman, A.E., Gordon, L.B., Gruenbaum, Y., Khuon, S., Mendez, M., Varga, R., and Collins, F.S. (2004). Accumulation of mutant lamin A causes progressive changes in nuclear architecture in Hutchinson-Gilford progeria syndrome. Proc. Natl. Acad. Sci. USA *101*, 8963–8968.

6. Pendás, A.M., Zhou, Z., Cadiñanos, J., Freije, J.M., Wang, J., Hultenby, K., Astudillo, A., Wernerson, A., Rodríguez, F., Tryggvason, K., and López-Otín, C. (2002). Defective prelamin A processing and muscular and adipocyte alterations in Zmpste24 metalloproteinase-deficient mice. Nat. Genet. *31*, 94–99.

7. Fong, L.G., Ng, J.K., Meta, M., Coté, N., Yang, S.H., Stewart, C.L., Sullivan, T., Burghardt, A., Majumdar, S., Reue, K., et al. (2004). Heterozygosity for Lmna deficiency eliminates the progeria-like phenotypes in Zmpste24-deficient mice. Proc. Natl. Acad. Sci. USA *101*, 18111–18116.

8. Leung, G.K., Schmidt, W.K., Bergo, M.O., Gavino, B., Wong, D.H., Tam, A., Ashby, M.N., Michaelis, S., and Young, S.G. (2001). Biochemical studies of Zmpste24-deficient mice. J. Biol. Chem. *276*, 29051–29058.

9. Capanni, C., Del Coco, R., Squarzoni, S., Columbaro, M., Mattioli, E., Camozzi, D., Rocchi, A., Scotlandi, K., Maraldi, N., Foisner, R., and Lattanzi, G. (2008). Prelamin A is involved in early steps of muscle differentiation. Exp. Cell Res. *314*, 3628–3637.

10. Favreau, C., Higuet, D., Courvalin, J.C., and Buendia, B. (2004). Expression of a mutant lamin A that causes Emery-Dreifuss muscular dystrophy inhibits in vitro differentiation of C2C12 myoblasts. Mol. Cell. Biol. *24*, 1481–1492.

11. Qu-Petersen, Z., Deasy, B., Jankowski, R., Ikezawa, M., Cummins, J., Pruchnic, R., Mytinger, J., Cao, B., Gates, C., Wernig, A., and Huard, J. (2002). Identification of a novel population of muscle stem cells in mice: potential for muscle regeneration. J. Cell Biol. *157*, 851–864.

12. Gharaibeh, B., Lu, A., Tebbets, J., Zheng, B., Feduska, J., Crisan, M., Péault, B., Cummins, J., and Huard, J. (2008). Isolation of a slowly adhering cell fraction containing stem cells from murine skeletal muscle by the preplate technique. Nat. Protoc. *3*, 1501–1509.

13. Lavasani, M., Lu, A., Thompson, S.D., Robbins, P.D., Huard, J., and Niedernhofer, L.J. (2013). Isolation of muscle-derived stem/progenitor cells based on adhesion characteristics to collagen-coated surfaces. Methods Mol. Biol. *976*, 53–65.

14. Peng, H., Wright, V., Usas, A., Gearhart, B., Shen, H.C., Cummins, J., and Huard, J. (2002). Synergistic enhancement of bone formation and healing by stem cell-expressed VEGF and bone morphogenetic protein-4. J. Clin. Invest. *110*, 751–759.

15. Payne, T.R., Oshima, H., Okada, M., Momoi, N., Tobita, K., Keller, B.B., Peng, H., and Huard, J. (2007). A relationship between vascular endothelial growth factor, angiogenesis, and cardiac repair after muscle stem cell transplantation into ischemic hearts. J. Am. Coll. Cardiol. *50*, 1677–1684.

16. Oshima, H., Payne, T.R., Urish, K.L., Sakai, T., Ling, Y., Gharaibeh, B., Tobita, K., Keller, B.B., Cummins, J.H., and Huard, J. (2005). Differential myocardial infarct repair with muscle stem cells compared to myoblasts. Mol. Ther. *12*, 1130–1141.

17. Lavasani, M., Robinson, A.R., Lu, A., Song, M., Feduska, J.M., Ahani, B., Tilstra, J.S., Feldman, C.H., Robbins, P.D., Niedernhofer, L.J., and Huard, J. (2012). Muscle-derived stem/progenitor cell dysfunction limits healthspan and lifespan in a murine progeria model. Nat. Commun. *3*, 608.

18. Rando, T.A. (2006). Stem cells, ageing and the quest for immortality. Nature *441*, 1080–1086.

19. Song, M., Lavasani, M., Thompson, S.D., Lu, A., Ahani, B., and Huard, J. (2013). Muscle-derived stem/progenitor cell dysfunction in Zmpste24-deficient progeroid mice limits muscle regeneration. Stem Cell Res. Ther. *4*, 33.

20. Niedernhofer, L.J., Garinis, G.A., Raams, A., Lalai, A.S., Robinson, A.R., Appeldoorn, E., Odijk, H., Oostendorp, R., Ahmad, A., van Leeuwen, W., et al. (2006). A new progeroid syndrome reveals that genotoxic stress suppresses the somatotroph axis. Nature *444*, 1038–1043.

21. Kim, D.H., Sarbassov, D.D., Ali, S.M., King, J.E., Latek, R.R., Erdjument-Bromage, H., Tempst, P., and Sabatini, D.M. (2002). mTOR interacts with raptor to form a nutrient-sensitive complex that signals to the cell growth machinery. Cell *110*, 163–175.

22. Saxton, R.A., and Sabatini, D.M. (2017). mTOR Signaling in Growth, Metabolism, and Disease. Cell *168*, 960–976.

23. Zoncu, R., Efeyan, A., and Sabatini, D.M. (2011). mTOR: from growth signal integration to cancer, diabetes and ageing. Nat. Rev. Mol. Cell Biol. *12*, 21–35.

24. Memmott, R.M., and Dennis, P.A. (2009). Akt-dependent and -independent mechanisms of mTOR regulation in cancer. Cell. Signal. *21*, 656–664.

25. Harrison, D.E., Strong, R., Sharp, Z.D., Nelson, J.F., Astle, C.M., Flurkey, K., Nadon, N.L., Wilkinson, J.E., Frenkel, K., Carter, C.S., et al. (2009). Rapamycin fed late in life extends lifespan in genetically heterogeneous mice. Nature *460*, 392–395.

26. Hansen, M., Chandra, A., Mitic, L.L., Onken, B., Driscoll, M., and Kenyon, C. (2008). A role for autophagy in the extension of lifespan by dietary restriction in C. elegans. PLoS Genet. *4*, e24.

27. Ramos, F.J., Chen, S.C., Garelick, M.G., Dai, D.F., Liao, C.Y., Schreiber, K.H., MacKay, V.L., An, E.H., Strong, R., Ladiges, W.C., et al. (2012). Rapamycin reverses elevated mTORC1 signaling in lamin A/C-deficient mice, rescues cardiac and skeletal muscle function, and extends survival. Sci. Transl. Med. *4*, 144ra103.

28. Takayama, K., Kawakami, Y., Lavasani, M., Mu, X., Cummins, J.H., Yurube, T., Kuroda, R., Kurosaka, M., Fu, F.H., Robbins, P.D., et al. (2017). mTOR signaling plays a critical role in the defects observed in muscle-derived stem/progenitor cells isolated from a murine model of accelerated aging. J. Orthop. Res. *35*, 1375–1382.

29. Bergo, M.O., Gavino, B., Ross, J., Schmidt, W.K., Hong, C., Kendall, L.V., Mohr, A., Meta, M., Genant, H., Jiang, Y., et al. (2002). Zmpste24 deficiency in mice causes spontaneous bone fractures, muscle weakness, and a prelamin A processing defect. Proc. Natl. Acad. Sci. USA *99*, 13049–13054.

30. Espada, J., Varela, I., Flores, I., Ugalde, A.P., Cadiñanos, J., Pendás, A.M., Stewart, C.L., Tryggvason, K., Blasco, M.A., Freije, J.M., and López-Otín, C. (2008). Nuclear envelope defects cause stem cell dysfunction in premature-aging mice. J. Cell Biol. *181*, 27–35.

31. Rossi, D.J., Bryder, D., Seita, J., Nussenzweig, A., Hoeijmakers, J., and Weissman, I.L. (2007). Deficiencies in DNA damage repair limit the function of haematopoietic stem cells with age. Nature *447*, 725–729.

32. Roobrouck, V.D., Ulloa-Montoya, F., and Verfaillie, C.M. (2008). Self-renewal and differentiation capacity of young and aged stem cells. Exp. Cell Res. *314*, 1937–1944.

33. Paulin, D., and Li, Z. (2004). Desmin: a major intermediate filament protein essential for the structural integrity and function of muscle. Exp. Cell Res. *301*, 1–7.

34. Chen, Q., Shou, P., Zheng, C., Jiang, M., Cao, G., Yang, Q., Cao, J., Xie, N., Velletri, T., Zhang, X., et al. (2016). Fate decision of mesenchymal stem cells: adipocytes or osteoblasts? Cell Death Differ. *23*, 1128–1139.

35. Laplante, M., and Sabatini, D.M. (2009). An emerging role of mTOR in lipid biosynthesis. Curr. Biol. *19*, R1046–R1052.

36. Wullschleger, S., Loewith, R., and Hall, M.N. (2006). TOR signaling in growth and metabolism. Cell *124*, 471–484.

37. Martin, D.E., and Hall, M.N. (2005). The expanding TOR signaling network. Curr. Opin. Cell Biol. *17*, 158–166.

38. Meng, D., Frank, A.R., and Jewell, J.L. (2018). mTOR signaling in stem and progenitor cells. Development *145*, dev152595.

39. Shiojima, I., Sato, K., Izumiya, Y., Schiekofer, S., Ito, M., Liao, R., Colucci, W.S., and Walsh, K. (2005). Disruption of coordinated cardiac hypertrophy and angiogenesis contributes to the transition to heart failure. J. Clin. Invest. *115*, 2108–2118.

40. Scaffidi, P., and Misteli, T. (2006). Lamin A-dependent nuclear defects in human aging. Science *312*, 1059–1063.

41. Haithcock, E., Dayani, Y., Neufeld, E., Zahand, A.J., Feinstein, N., Mattout, A., Gruenbaum, Y., and Liu, J. (2005). Age-related changes of nuclear architecture in Caenorhabditis elegans. Proc. Natl. Acad. Sci. USA *102*, 16690–16695.

42. Vazquez, A., Bond, E.E., Levine, A.J., and Bond, G.L. (2008). The genetics of the p53 pathway, apoptosis and cancer therapy. Nat. Rev. Drug Discov. *7*, 979–987.

43. Niedernhofer, L.J., and Robbins, P.D. (2008). Signaling mechanisms involved in the response to genotoxic stress and regulating lifespan. Int. J. Biochem. Cell Biol. *40*, 176–180.

44. Chen, C., Liu, Y., Liu, Y., and Zheng, P. (2009). mTOR regulation and therapeutic rejuvenation of aging hematopoietic stem cells. Sci. Signal. *2*, ra75.

45. Chen, C., Liu, Y., Liu, R., Ikenoue, T., Guan, K.L., Liu, Y., and Zheng, P. (2008). TSC-mTOR maintains quiescence and function of hematopoietic stem cells by repressing mitochondrial biogenesis and reactive oxygen species. J. Exp. Med. *205*, 2397–2408.

46. Cho, J.S., Kook, S.H., Robinson, A.R., Niedernhofer, L.J., and Lee, B.C. (2013). Cell autonomous and nonautonomous mechanisms drive hematopoietic stem/progenitor cell loss in the absence of DNA repair. Stem Cells *31*, 511–525.

47. Menendez, J.A., Vellon, L., Oliveras-Ferraros, C., Cufí, S., and Vazquez-Martin, A. (2011). mTOR-regulated senescence and autophagy during reprogramming of somatic cells to pluripotency: a roadmap from energy metabolism to stem cell renewal and aging. Cell Cycle *10*, 3658–3677.

48. He, X., Song, W., Liu, C., Chen, S., and Hua, J. (2014). Rapamycin inhibits acrolein-induced apoptosis by alleviating ROS-driven mitochondrial dysfunction in male germ cells. Cell Prolif. *47*, 161–171.

49. Luo, Y., Li, L., Zou, P., Wang, J., Shao, L., Zhou, D., and Liu, L. (2014). Rapamycin enhances long-term hematopoietic reconstitution of ex vivo expanded mouse hematopoietic stem cells by inhibiting senescence. Transplantation *97*, 20–29.

50. Zhang, Y.H., Lin, Q.F., Wang, X.L., Li, Q.Y., Chai, J.J., and Fan, X.J. (2017). Rapamycin induces human acute promyelocytic leukemia cell HL-60 autophagic apoptosis. Eur. Rev. Med. Pharmacol. Sci. *21*, 5506–5514.

51. Villeda, S.A., Luo, J., Mosher, K.I., Zou, B., Britschgi, M., Bieri, G., Stan, T.M., Fainberg, N., Ding, Z., Eggel, A., et al. (2011). The ageing systemic milieu negatively regulates neurogenesis and cognitive function. Nature *477*, 90–94.

52. Greising, S.M., Call, J.A., Lund, T.C., Blazar, B.R., Tolar, J., and Lowe, D.A. (2012). Skeletal muscle contractile function and neuromuscular performance in *Zmpste24* $^{-/-}$ mice, a murine model of human progeria. Age (Dordr.) *34*, 805–819.

53. Varga, R., Eriksson, M., Erdos, M.R., Olive, M., Harten, I., Kolodgie, F., Capell, B.C., Cheng, J., Faddah, D., Perkins, S., et al. (2006). Progressive vascular smooth muscle cell defects in a mouse model of Hutchinson-Gilford progeria syndrome. Proc. Natl. Acad. Sci. USA *103*, 3250–3255.

54. Scaffidi, P., and Misteli, T. (2008). Lamin A-dependent misregulation of adult stem cells associated with accelerated ageing. Nat. Cell Biol. *10*, 452–459.

55. von Maltzahn, J., Chang, N.C., Bentzinger, C.F., and Rudnicki, M.A. (2012). Wnt signaling in myogenesis. Trends Cell Biol. *22*, 602–609.

56. Chakkalakal, J.V., Jones, K.M., Basson, M.A., and Brack, A.S. (2012). The aged niche disrupts muscle stem cell quiescence. Nature *490*, 355–360.

57. Li, C.J., Madhu, V., Balian, G., Dighe, A.S., and Cui, Q. (2015). Cross-Talk Between VEGF and BMP-6 Pathways Accelerates Osteogenic Differentiation of Human Adipose-Derived Stem Cells. J. Cell. Physiol. *230*, 2671–2682.

58. Li, P., Bai, Y., Yin, G., Pu, X., Huang, Z., Liao, X., Chen, X., and Yao, Y. (2014). Synergistic and sequential effects of BMP-2, bFGF and VEGF on osteogenic differentiation of rat osteoblasts. J. Bone Miner. Metab. *32*, 627–635.

59. Zhang, L.F., Qi, J., Zuo, G., Jia, P., Shen, X., Shao, J., Kang, H., Yang, H., and Deng, L. (2014). Osteoblast-secreted factors promote proliferation and osteogenic differentiation of bone marrow stromal cells via VEGF/heme-oxygenase-1 pathway. PLoS ONE *9*, e99946.

60. Xue, Q., Nagy, J.A., Manseau, E.J., Phung, T.L., Dvorak, H.F., and Benjamin, L.E. (2009). Rapamycin inhibition of the Akt/mTOR pathway blocks select stages of VEGF-A164-driven angiogenesis, in part by blocking S6Kinase. Arterioscler. Thromb. Vasc. Biol. *29*, 1172–1178.

61. Hara, K., Yonezawa, K., Kozlowski, M.T., Sugimoto, T., Andrabi, K., Weng, Q.P., Kasuga, M., Nishimoto, I., and Avruch, J. (1997). Regulation of eIF-4E BP1 phosphorylation by mTOR. J. Biol. Chem. *272*, 26457–26463.

62. Burnett, P.E., Barrow, R.K., Cohen, N.A., Snyder, S.H., and Sabatini, D.M. (1998). RAFT1 phosphorylation of the translational regulators p70 S6 kinase and 4E-BP1. Proc. Natl. Acad. Sci. USA *95*, 1432–1437.

63. Ma, X.M., and Blenis, J. (2009). Molecular mechanisms of mTOR-mediated translational control. Nat. Rev. Mol. Cell Biol. *10*, 307–318.

64. Cao, K., Graziotto, J.J., Blair, C.D., Mazzulli, J.R., Erdos, M.R., Krainc, D., and Collins, F.S. (2011). Rapamycin reverses cellular phenotypes and enhances mutant protein clearance in Hutchinson-Gilford progeria syndrome cells. Sci. Transl. Med. *3*, 89ra58.

65. Blagosklonny, M.V. (2011). Progeria, rapamycin and normal aging: recent breakthrough. Aging (Albany N.Y.) *3*, 685–691.

66. Cenni, V., Capanni, C., Columbaro, M., Ortolani, M., D'Apice, M.R., Novelli, G., Fini, M., Marmiroli, S., Scarano, E., Maraldi, N.M., et al. (2011). Autophagic degradation of farnesylated prelamin A as a therapeutic approach to lamin-linked progeria. Eur. J. Histochem. *55*, e36.

67. Evangelisti, C., Cenni, V., and Lattanzi, G. (2016). Potential therapeutic effects of the MTOR inhibitors for preventing ageing and progeria-related disorders. Br. J. Clin. Pharmacol. *82*, 1229–1244.

68. Cravedi, P., Ruggenenti, P., and Remuzzi, G. (2009). Sirolimus to replace calcineurin inhibitors? Too early yet. Lancet *373*, 1235–1236.

69. Wang, B., Lin, Y., Hu, Y., Shan, W., Liu, S., Xu, Y., Zhang, H., Cai, S., Yu, X., Cai, Z., and Huang, H. (2017). mTOR inhibition improves the immunomodulatory properties of human bone marrow mesenchymal stem cells by inducing COX-2 and PGE_2. Stem Cell Res. Ther. *8*, 292.

70. Lynch, C.J. (2001). Role of leucine in the regulation of mTOR by amino acids: revelations from structure-activity studies. J. Nutr. *131*, 861S–865S.

71. Zaytseva, Y.Y., Valentino, J.D., Gulhati, P., and Evers, B.M. (2012). mTOR inhibitors in cancer therapy. Cancer Lett. *319*, 1–7.

72. Kofman, A.E., McGraw, M.R., and Payne, C.J. (2012). Rapamycin increases oxidative stress response gene expression in adult stem cells. Aging (Albany N.Y.) *4*, 279–289.

73. Robida-Stubbs, S., Glover-Cutter, K., Lamming, D.W., Mizunuma, M., Narasimhan, S.D., Neumann-Haefelin, E., Sabatini, D.M., and Blackwell, T.K. (2012). TOR signaling and rapamycin influence longevity by regulating SKN-1/Nrf and DAF-16/FoxO. Cell Metab. *15*, 713–724.

74. Matsuzaki, T., Matsushita, T., Takayama, K., Matsumoto, T., Nishida, K., Kuroda, R., and Kurosaka, M. (2014). Disruption of Sirt1 in chondrocytes causes accelerated progression of osteoarthritis under mechanical stress and during ageing in mice. Ann. Rheum. Dis. *73*, 1397–1404.

75. Shoji, T., Ii, M., Mifune, Y., Matsumoto, T., Kawamoto, A., Kwon, S.M., Kuroda, T., Kuroda, R., Kurosaka, M., and Asahara, T. (2010). Local transplantation of human multipotent adipose-derived stem cells accelerates fracture healing via enhanced osteogenesis and angiogenesis. Lab. Invest. *90*, 637–649.

76. Johnstone, B., Hering, T.M., Caplan, A.I., Goldberg, V.M., and Yoo, J.U. (1998). In vitro chondrogenesis of bone marrow-derived mesenchymal progenitor cells. Exp. Cell Res. *238*, 265–272.

77. Schon, B.S., Schrobback, K., van der Ven, M., Stroebel, S., Hooper, G.J., and Woodfield, T.B. (2012). Validation of a high-throughput microtissue fabrication process for 3D assembly of tissue engineered cartilage constructs. Cell Tissue Res. *347*, 629–642.

78. Schneider, C.A., Rasband, W.S., and Eliceiri, K.W. (2012). NIH Image to ImageJ: 25 years of image analysis. Nat. Methods *9*, 671–675.

79. Zuk, P.A., Zhu, M., Mizuno, H., Huang, J., Futrell, J.W., Katz, A.J., Benhaim, P., Lorenz, H.P., and Hedrick, M.H. (2001). Multilineage cells from human adipose tissue: implications for cell-based therapies. Tissue Eng. *7*, 211–228.

80. Ramírez-Zacarías, J.L., Castro-Muñozledo, F., and Kuri-Harcuch, W. (1992). Quantitation of adipose conversion and triglycerides by staining intracytoplasmic lipids with Oil red O. Histochemistry *97*, 493–497.